Available online at www.sciencedirect.com
ScienceDirect
Ocean Engineering 34 (2007) 1977–1994
OCEAN ENGINEERING
www.elsevier.com/locate/oceaneng

The effect of directionality on extreme wave design criteria

Philip Jonathan[a], Kevin Ewans[b,*]

[a]Shell Research Limited, P.O. Box 1, Chester, UK
[b]Shell International Exploration and Production, P.O. Box 60, 2280 AB Rijswijk, The Netherlands

Received 4 December 2006; accepted 8 March 2007
Available online 16 March 2007

Abstract

Sea state design criteria for offshore facilities are frequently provided by direction. For example, it is typical for return-period values of the significant wave height to be specified for each of eight 45° sectors in addition to the omni-directional case. However, it is important that these criteria be consistent so that the probability of exceedance of a given wave height from any direction derived from the directional values is the same as for the omni-directional value. As recently demonstrated by Forristall it is not sufficient simply to scale the directional values so that the value of the wave height from the most severe sector is the same as the omni-directional value.

We develop an approach for establishing appropriate directional criteria and an associated omni-directional criterion for a specific location. The inherent directionality of sea states is used to develop a model for the directional dependence of distributions of storm maxima. The directional model is applied to the GOMOS data, and the distributional properties of the 100-year significant wave height are estimated and the implications for design discussed. An objective risk-cost approach is proposed for optimising directional criteria, while preserving overall reliability. Simulation studies are performed, using realistic extreme value assumptions, to quantify the uncertainties.

Keywords: Wave height; Gulf of Mexico; Wave direction; Extreme; Design; Risk; Hurricane

1. Introduction

Environmental design criteria for offshore facilities have inherent uncertainties. These are functions of climate variability in time and space, and storm peak direction and track. The quality of estimation of design criteria is further dependent on inherent data quality and sample size.

In a previous study (Elsinghorst et al., 1998), application of Generalised Pareto modelling to estimation of North Sea storm severity is reported for storms with return periods of 100–500 years based on NESS hindcast data. The study consisted of the following elements. The tail distribution of storm severity was modelled and magnitudes of extreme events with long return periods estimated. Uncertainty of estimates was quantified using a bootstrapping approach. Bias and coverage for estimates of uncertainty were quantified by simulation study.

Site averaging can be used to increase the sample size for modelling, and to account for randomness of storm track, in hurricane-dominated regions (Forristall et al., 1991). However, hurricane data from relatively largely separated locations are highly correlated. Thus careful quantification of uncertainty of parameter estimates and extreme quantiles is necessary, accommodating this dependency structure. Jonathan and Ewans (2006) adopt a bootstrapping approach to calculate interval estimates for GPD model parameters and extreme quantiles to account for spatial dependence of extremes when site averaging is used.

In most regions, but particularly hurricane-dominated regions (e.g. Gulf of Mexico), and in regions where extra-tropical storms prevail (e.g. Northern North Sea), extremal properties of storms are dependent on storm direction. Accordingly, sea state design criteria for offshore facilities are frequently provided by direction, to optimise

*Corresponding author.
E-mail addresses: philip.jonathan@shell.com (P. Jonathan), kevin.ewans@shell.com (K. Ewans).

0029-8018/$ - see front matter © 2007 Elsevier Ltd. All rights reserved.
doi:10.1016/j.oceaneng.2007.03.003

engineering facilities for the directional environment. For example, return-period values of the significant wave height can be specified for each of eight 45° sectors in addition to the omni-directional case. However, debate continues (e.g. Forristall, 2004) on how these should be derived in a consistent way. This article proposes a method for developing criteria for directional environments.

Theory and application of extreme value modelling is summarised, for example, by Kotz and Nadarajah (2000) and Reiss and Thomas (2001). The former authors provide an interesting overview of applications including those of Coles, Tawn and co-workers. For example, Coles and Walshaw (1994) model extremal properties of wind speeds as a function of their direction, accounting during fitting for angular-dependency structure, by inflating standard errors for parameter estimates. Robinson and Tawn (1997) apply a Fourier model to characterise the extremal behaviour of sea currents. Coles and Powell (1996) discuss a Bayesian approach to extreme value estimation using data from multiple locations. Coles and Casson (1998), Casson and Coles (1999) present spatial models for extremes. Coles and Tawn (1996, 2005) discuss the estimation of predictive distributions (for quantities such as H_{S100}), which incorporate uncertainties in model parameters. There are numerous recent articles in the offshore engineering literature (e.g. Arena et al., 2006) that refer to estimation of directional extremes.

The paper is arranged as follows. In Section 2, we introduce the GOMOS hindcast data motivating the investigation, illustrating some key features. In Section 3, an outline of the generalised Pareto distribution (GPD) used to characterise the extreme value behaviour of the data is given. We also present a directional model for the parameters of the GPD distribution, and outline the application of maximum likelihood to estimate paremeters of the directional model, and their uncertainties. Further detail of the maximum likelihood estimation is given in Appendix A. We then apply the directional model to the GOMOS data. In Section 4, we extend the model to estimate distributional properties of 100-year significant wave height H_{S100} and illustrate our findings using GOMOS. In Section 5, we discuss estimation of design criteria in the presence of directional dependence, and evaluate implications for designs at GOMOS. In Section 6, we summarise findings and make suggestions and recommendations for future studies.

2. Data

The data examined are significant wave height, H_S values from the proprietary GOMOS Gulf of Mexico hindcast Study (Oceanweather, 2005), for the period September 1900 to September 2005 inclusive, at 30-min intervals. For a typical Gulf of Mexico region, we selected 120 grid points arranged on a 15×8 rectangular lattice with spacing with 0.125° (14 km). For each storm period for each grid point, we isolated storm peak significant wave height, H_S^{SP}, for modelling purposes, together with the corresponding wave direction at storm peak H_S, henceforth referred to as storm peak direction. Thus, extreme value modelling is performed on storm peak wave height data (one value for each storm at each of 120 locations, giving approximately 315 storm peak values for each location in the period 1900–2005).

Fig. 1 shows H_S^{SP} as a function of storm peak direction for all locations. Storm peak direction is defined clockwise from the North. It is apparent that storms are more frequent in sector [0, 180], which also contains the highest

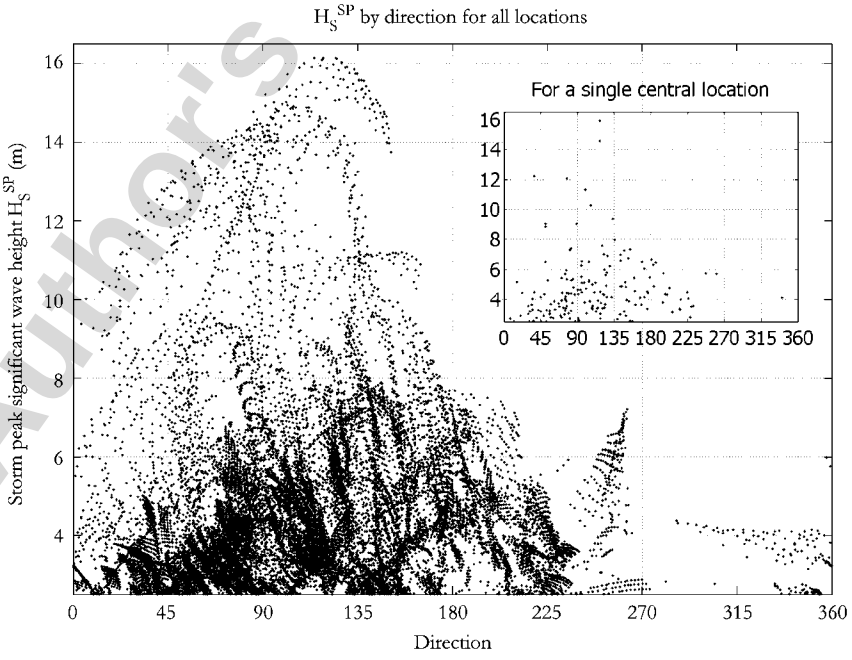

Fig. 1. Storm peak significant wave height H_S^{SP} above a threshold of 2.5 m as a function of direction for all locations. Inset: H_S^{SP} by direction for a single central location.

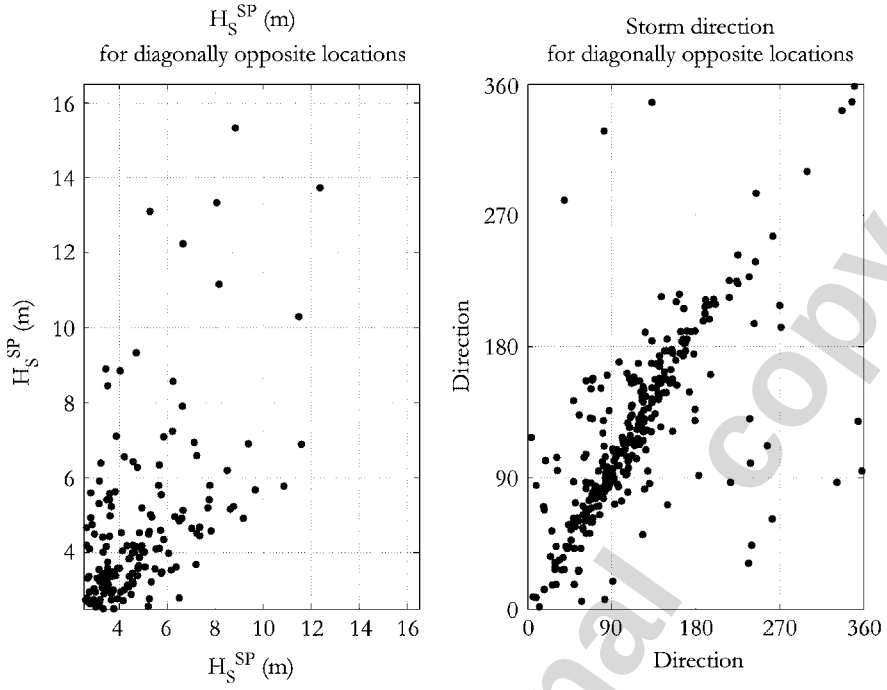

Fig. 2. Scatter plot to illustrate dependence of storm peak significant wave height H_S^{SP} and storm peak direction for diagonally opposite locations, approximately 150 km apart.

values of H_S^{SP}. Storms are relatively infrequent in $[270, 360]$. Inset in Fig. 1 is the corresponding data for a single central location. Fig. 2 illustrates the extent of dependence between storm peak H_S and storm direction. For a pair of locations, corresponding to diagonally opposite corners of the 15×8 grid of locations (approximately 150 km apart), scatter plots show paired values of storm peak H_S per storm (left-hand side) and storm direction (right-hand side). It is clear that storm peak H_S and storm direction are dependent.

Storm events do not correspond to a single wave direction only. For a given storm event, 30-min sea states extend over a range of wave directions in general. Nevertheless, for extreme value analysis, we characterise a storm in terms of its storm peak significant wave height, H_S^{SP} and storm peak direction. However, in estimating directional design criteria, we also account for the influence of storms over their full range of sea states and wave directions, by estimating the directional dissipation of sea-states of storms as a function of angular distance from storm peak direction. Fig. 3 gives the median directional storm dissipation ρ as a function of H_S^{SP}. For any storm, ρ is the minimum reduction in H_S (expressed as a fraction of H_S^{SP}) as a function of angular difference from storm peak direction. Directional dissipation will be discussed further and applied in Section 4.

3. Modelling extremal properties incorporating directionality

Suppose we have values for storm peak significant wave heights $\{X_i\}_{i=1}^n$ and corresponding storm peak directions $\{\theta_i\}_{i=1}^n$ for a set of n storm events occurring in period P_0. We assume, for any storm, that the distribution of extreme wave heights above a certain threshold u can be described using the GPD with cumulative distribution function $F_{X_i|\theta_i,u}$ given by

$$F_{X_i|\theta_i,u}(x) = P(X_i \leqslant x|\theta_i, u),$$
$$= 1 - \left(1 + \frac{\gamma(\theta_i)}{\sigma(\theta_i)}(x-u)\right)_+^{-\frac{1}{\gamma(\theta_i)}},$$
$$\text{for } x > u,\ \sigma > 0,$$

where γ is the shape parameter or tail index, σ the scale, both of which are functions of storm peak direction θ_i. The extreme value threshold u is assumed constant with respect to direction. We assume that, per location, the set $\{X_i\}_{i=1}^n$ consists of independent random variables, and note that the notation $a_+ = \max(a, 0)$ is used. Pickands (1975) showed, for sufficiently high threshold u, that the GPD provides a good representation for any distribution function $G_{X_i|\theta_i,u}$, in the sense that

$$\lim_{u \to x_o} \sup_{0 < x < x_o - u} \left| G_{X_i|\theta_i,u} - F_{X_i|\theta_i,u} \right| = 0,$$

where x_o is the upper tail point of $F_{X_i|\theta_i,u}$.

In common with other authors (e.g. Robinson and Tawn, 1997), since we expect the extreme value parameters γ and σ to vary smoothly with direction, we characterise their directional dependence using a Fourier series expansion $\sum_{k=0}^{p} \sum_{b=1}^{2} A_{abk} t_b(k\theta)$, where $t_1 = \cos$, $t_2 = \sin$, with $a = 1$ for γ, and $a = 2$ for σ. We set $A_{a20} = 0$, $a = 1, 2$ since this parameter is indeterminate. p is the order of the

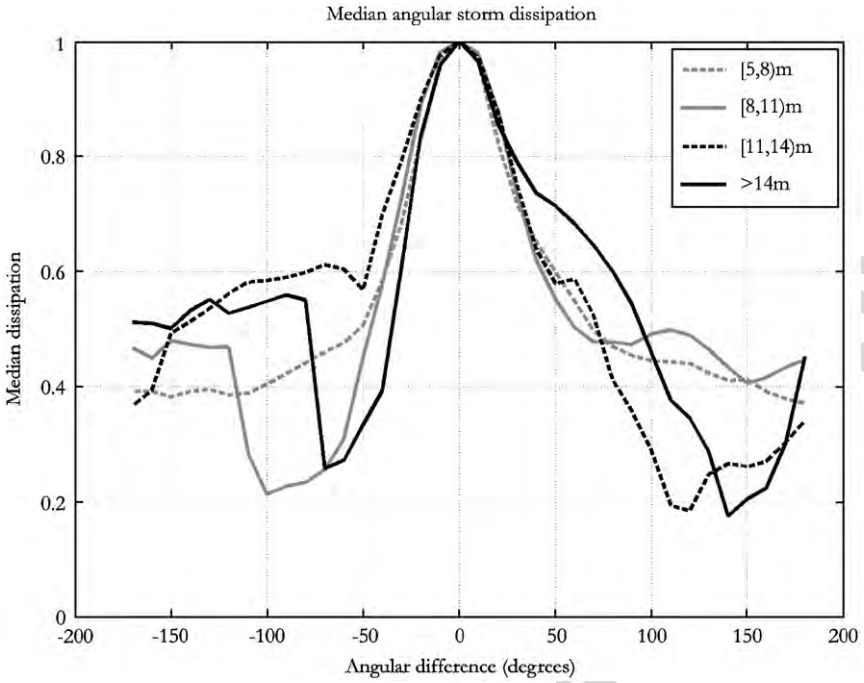

Fig. 3. Median directional storm dissipation ρ as a function of H_S^{SP}. For any storm, ρ is the minimum reduction in H_S (expressed as a fraction of H_S^{SP}) as a function of angular difference from the storm peak direction.

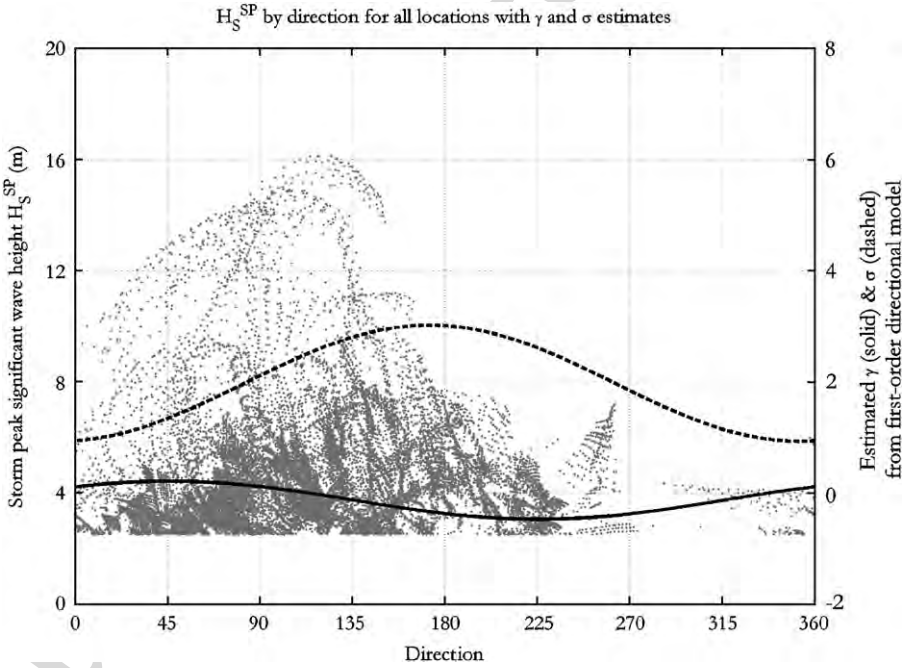

Fig. 4. First-order directional model applied to GOMOS data for all locations. Figure shows H_S^{SP} and estimated γ and σ as a function of storm peak direction.

Fourier model, $p = 0$ corresponding to a constant model. Thus, for example, we refer to the cases $p = 1$ and 3 as first- and third-order directional models, respectively. We estimate the parameters A_{110}, A_{210}, A_{abk}, $a = 1, 2$, $b = 1, 2$, $k = 1, 2, \ldots, p$ using maximum likelihood estimation as explained in Appendix A. The first-order directional model, when applied to the GOMOS data for all 120 locations, yields the functional relationships:

$$\gamma = -0.13 + 0.24\cos(\theta) + 0.24\sin(\theta),$$
$$\sigma = 1.97 - 1.04\cos(\theta) + 0.14\sin(\theta),$$

for γ and σ with direction, illustrated in Fig. 4 with the H_S^{SP} data for comparison. Fig. 5 compares the functional forms

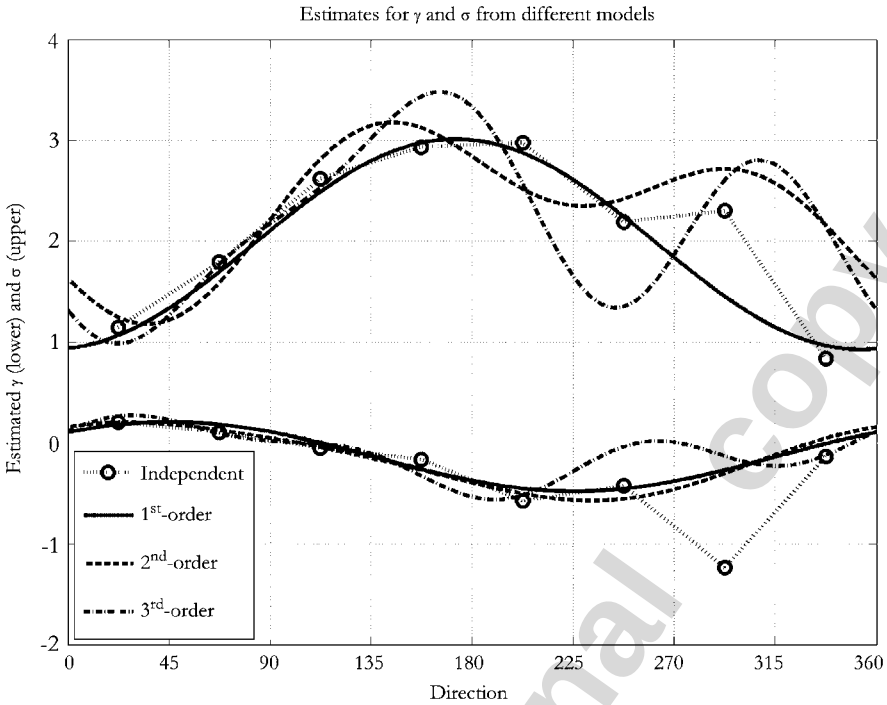

Fig. 5. First-, second- and third-order directional models for GOMOS data for all locations. Also shown are independent estimates for γ and σ calculated using data from consecutive directional sectors of width 45°. The corresponding zero-order (constant) estimates for γ and σ are respectively −0.019 and 2.22.

of γ and σ with storm peak direction for first-, second- and third-order models. Also given in Fig. 5 are estimates found independently using data from consecutive directional sectors of width 45°. The directional model produces smooth estimates that are broadly consistent with independent fits. From Fig. 5 we judge that the first-order model adequately characterises the variability of extreme value parameters with storm peak direction, while noting that more formal model selection procedures might be useful in practice. Clearly the most appropriate model order depends on the characteristics of the data; higher order models might be necessary for locations with more complex directional dependence.

We note that many different approaches exist to estimate an appropriate level of directional complexity for the Fourier model. In this work, we restrict our attention to a first-order Fourier model, having demonstrated it provides a better characterisation of the data than a constant model. In another application to North Sea storms (Ewans and Jonathan, 2007), a high-order Fourier form ensures the directional extreme value model is sufficiently flexible to characterise variation in extremal behaviour with storm direction. However, a roughness penality is imposed to ensure that extreme value estimates are as smooth as possible, consistent with the data within a maximum likelihood framework. Cross-validation is used to estimate the appropriate roughness penalty.

Given the Fourier series expressions for γ and σ, we estimate asymptotic variances for these parameters as explained in Appendix A. Asymptotic 95% confidence bands for γ and σ with direction are given in Fig. 6. Lines representing the asymptotic limits are barely distinguishable from those representing maximum likelihood estimates.

When spatial dependence is present, bootstrapping can be used to estimate more realistic interval estimates for model parameters. Bootstrapping involves estimating parameter uncertainty by resampling the original data sample (e.g. Hall, 1988, Efron and Tibshirani, 1993, Davison and Hinkley, 1997). Coles and Simiu (2003) discuss difficulties in applying bootstrapping for estimation of uncertainties in extreme value analysis, including a tendency to underestimate extreme quantiles. Nevertheless, they conclude that bootstrapping, carefully applied, can be used reliably to give realistic estimates for parameter uncertainties. Heffernan and Tawn (2004) report a conditional approach for extreme value analysis applicable to higher dimensional problems, also incorporating bootstrapping, in which dependence structure is characterised using rank correlation. Using the studentised non-parametric bootstrap discussed by Jonathan and Ewans (2006), we estimate bootstrap 95% confidence intervals for the parameters $\{A_{abk}\}_{a=1,b=1,k=0}^{2,2,p}$, γ and σ. We are careful to preserve dependency structure between locations; data for all locations for any given storm is treated as a single multivariate observation for resampling. Bootstrap 95% intervals for A_{abk}, assuming first-order models for each of γ and σ, based on 500 storm-wise resamples of H_S^{SP} data are given in Table 1. Corresponding bootstrap 95% intervals for γ and σ are shown in Fig. 6.

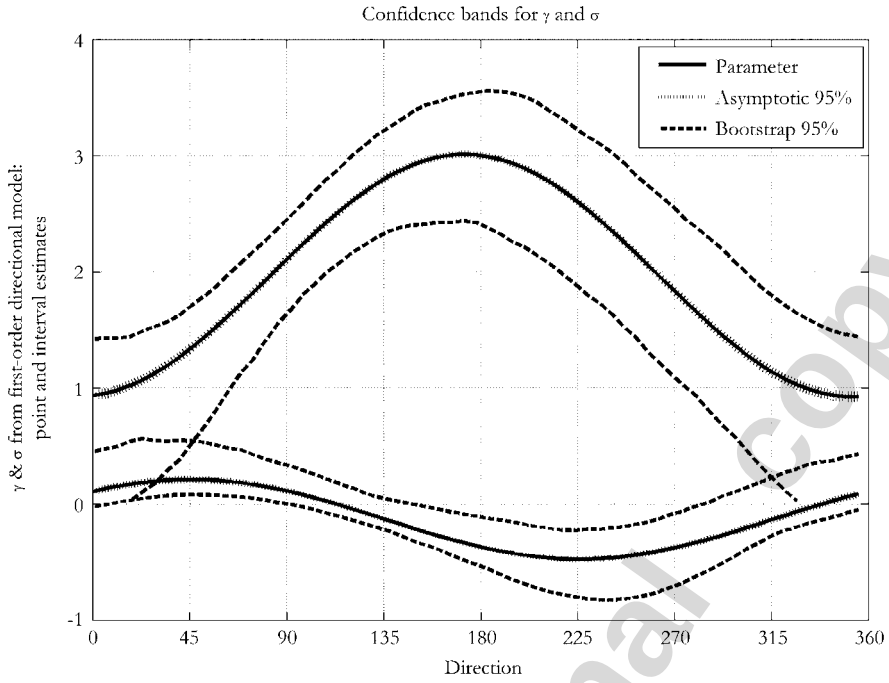

Fig. 6. Point and interval estimates for γ and σ with storm peak direction.

Table 1
Point and interval estimates for first-order model parameters

Parameter	Estimate	Asymptotic 95%	Bootstrap 95%
A_{110}	−0.13	(−0.14, −0.13)	(−0.25, 0.06)
A_{111}	0.24	(0.23, 0.25)	(0.10, 0.48)
A_{121}	0.24	(0.24, 0.25)	(0.09, 0.44)
A_{210}	1.97	(1.95, 1.98)	(1.59, 2.30)
A_{211}	−1.04	(−1.05, −1.02)	(−1.76, −0.60)
A_{221}	0.14	(0.12, 0.15)	(−0.31, 0.62)

Some technical details of the bootstrapping analysis need to be noted. For each of the 500 bootstrap resamples, a likelihood ratio test was performed to check that the first-order model (for both of γ and σ) could be justified over the corresponding constant model. Specifically, twice the difference of the negative log-likelihoods (known as "deviance") is compared with the critical value of the χ^2 distribution with 4 degrees of freedom (since the first-order model has four more parameters that the constant model). Approximately 20 resamples for which the first-order model was rejected were ignored for estimation of asymptotics. Further, as can be seen from Fig. 6, the value of γ approaches -0.5 for some storm peak directions, causing numerical difficulties (because of the requirement of $\gamma > -0.5$) for estimation of asymptotic variances. To overcome this difficulty, we replace the term in $(1+2\gamma)$ in the expressions for elements of the information matrix by 0.2 for all $\gamma < -0.4$. Initial checks suggest that this approximation is reasonable. Appendix B confirms the approximation provides interval estimates with reasonable coverage probabilities.

From the table and figure it can be seen that asymptotic statistics greatly underestimate uncertainties of parameters. Bootstrapping provides more realistic interval estimates. The bootstrap 95% interval for γ is always positive for some storm peak directions, and always negative for others, demonstrating the presence of directionally dependent extremes.

4. Estimation of omni-directional extremes

We assume that occurrences of storms are independent Poisson events with expectation $1/P_0$ per annum per storm, where P_0 is the period of hindcast data. We further assume that the empirical distribution of storm peak directions given by the set $\{\theta_i\}_{i=1}^n$ provides an adequate representation of the distribution of storm peak directions for any period P of interest; that is, storm peak directions for any P are restricted to the set $\{\theta_i\}_{i=1}^n$. Robinson and Tawn (1997) and Chavez-Demoulin and Davison (2005) present a series of models of varying complexity appropriate for the current situation.

Using the directional model introduced above, we estimate the cumulative distribution function of the maximum storm H_S for an arbitrary directional sector S, corresponding to period P. When this period is 100 years, we will refer to this as H_{S100}. We consider the influence of storm events, the storm peak directions of which correspond to the sector S, and the influence of all other storm events on the sector, even though their storm peak directions fall outside S. This effect is illustrated in Fig. 7, which shows H_S versus wave direction for consecutive 30-min sea states of a typical storm at a typical location. From Fig. 7, we see that H_S^{SP} corresponds to a

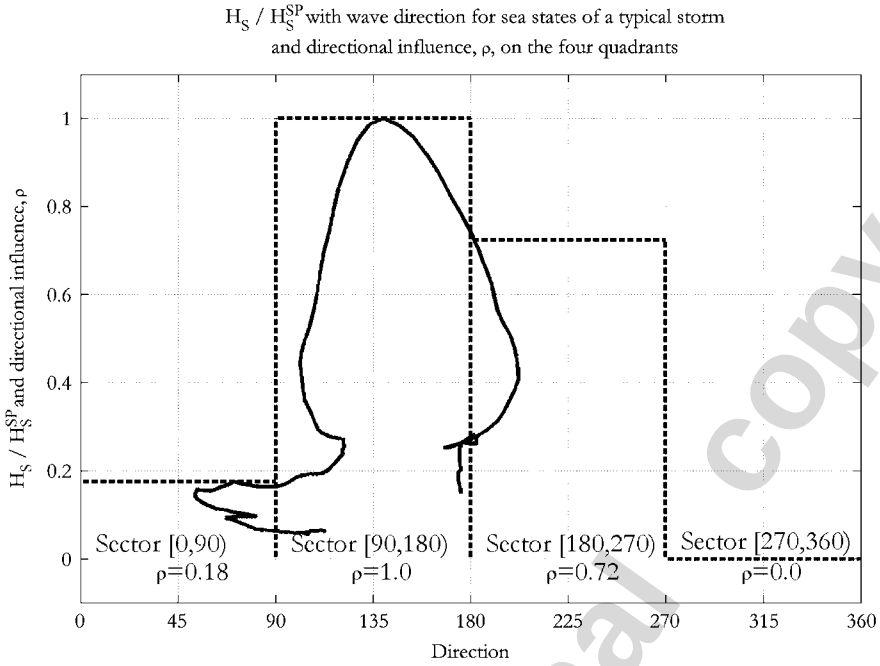

Fig. 7. Variation of H_S/H_S^{SP} with wave direction (solid) for 30-min sea states of a typical storm. H_S^{SP} corresponds to a storm peak direction of approximately 140°, but sea states extend over a wide range of wave directions. Also shown (dashed) is the directional influence of the storm on each of the four quadrants.

wave direction of approximately 140°, but that sea states extend over a wide range of wave directions. To establish design criteria for the first directional quadrant $[0, 90)$, we quantify the contribution of the storm to that sector in terms of the maximum value of sea state H_S (expressed as a fraction of H_S^{SP}) for any sea state whose wave direction falls within the sector. In general, we refer to this quantity as the directional influence $\rho_i(S)$ of storm i on sector S. Thus, for the storm in Fig. 7, the directional influence of the storm on sector $[0, 90)$ is approximately 0.18. Similarly, the directional influence of the storm on quadrant $[90, 180)$ is unity (since storm peak direction corresponds to this sector). The directional influence of the storm on quadrant $[270, 360]$ is zero, since no sea states of the storm fall in this sector.

Directional influence quantifies the maximum contribution of a storm to a directional sector as a fraction of storm peak H_S. From the GOMOS data, we can extract values for directional influence to facilitate estimation of maximum storm H_S for any storm-sector combination of interest. We characterise the extremal behaviour of X_i, the value of H_S^{SP} for the ith storm given its storm peak direction, using the directional model from above, where X_i is GPD-distributed. The contribution of this storm event to any directional sector S is quantified in terms of the random variable $\rho_i(S)X_i$, namely the maximum contribution of the storm to the sector observed in the 105 years of GOMOS data. Since the storm events are statistically independent, we proceed to calculate the statistical properties of the maximum storm H_S in an arbitrary sector S as follows.

In any period P, the cumulative distribution function of the maximum storm H_S in sector S, $X_{\max S}$, is given by

$$\begin{aligned} F_{X_{\max S}}(x) &= P(X_{\max S} \leqslant x | X_i > u \forall i, \quad i \in [1, 2, \ldots, n]), \\ &= \prod_{i=1}^{n} \left\{ \sum_{k=0}^{\infty} P\left(\rho_i(S) X_i \leqslant x | X_i > u, \quad M_i = k\right) \right. \\ &\quad \left. \times P(M_i = k) \right\}, \end{aligned}$$

where M_i is the number of occurrences of storm i in the period, the expected value of which is $m = P/P_0$ for all storms. Recalling that M_i is Poisson distributed, we have

$$\begin{aligned} &F_{X_{\max S}}(x) \\ &= \prod_{i=1}^{n} \left\{ \sum_{k=0}^{\infty} \left(1 - \left(1 + \frac{\gamma(\theta_i)}{\sigma(\theta_i)} \left(\frac{x}{\rho_i(S)} - u \right) \right)_+^{-\frac{1}{\gamma(\theta_i)}} \right)^k \frac{e^{-m} m^k}{k!} \right\}, \\ &= \exp\left\{ -m \sum_{i=1}^{n} \left(1 + \frac{\gamma(\theta_i)}{\sigma(\theta_i)} \left(\frac{x}{\rho_i(S)} - u \right) \right)_+^{-\frac{1}{\gamma(\theta_i)}} \right\}. \end{aligned}$$

Note, in particular, that if this sector was homogeneous so that $\gamma(\theta_i) = \gamma_S$, $\sigma(\theta_i) = \sigma_S$, and further if $\rho_i(S) = 1$, $\forall i$, then this expression would reduce to the standard GEV

$$\exp\left\{ -m n_S \left(1 + \frac{\gamma_S}{\sigma_S}(x - u) \right)_+^{-\frac{1}{\gamma_S}} \right\},$$

where $m n_S$ is the expected number of storms in the sector in period P, n_S being the number of storms in S in P_0 (see, e.g. Coles and Walshaw (1994)). Leadbetter et al. (1983) give

the theoretical framework within which modelling maxima using GEV are valid.

Once values of $\{\gamma(\theta_i), \sigma(\theta_i)\}_{i=1}^{n}$ have been estimated, the distribution of H_{S100}, the $P = 100$ year maximum, is estimated by setting the expression for $F_{X_{\max S}}(x) = q$ for any quantile q, $q \in [0, 1]$, and setting $P = 100$ years, then solving for x for an arbitrary sector. The most probable value $H_{S100\,\mathrm{MP}}$ of H_{S100} is estimated by setting the second derivative of $F_{X_{\max S}}(x)$ to zero and solving for x.

We calculate cumulants for sector maxima for the four quadrants ([0, 90), [90, 180), [180, 270) and [270, 360)) and for the omni-directional (i.e. for sector [0, 360)) case for the GOMOS data. The resulting cumulative distribution functions for H_{S100} are given in Fig. 8 for the directional model (using first-order models for each of γ and σ). Given we have observed that directional effects influence extreme storm behaviour for these data, we expect differences between sector cumulants. Sectors [0, 90) and [90, 180) show much longer, heavier tails.

For comparison, we show corresponding cumulants (Fig. 9) based on the direction-independent EV model (assuming γ and σ constant and independent of storm peak direction). Cumulants based on the directional model describe the data more accurately, notwithstanding the uncertainties in model parameters already discussed. We note that the omni-directional cumulant based on the directional model has a longer and heavier right-hand tail, indicating that large values of H_{S100} are more likely than we might anticipate were we to base our beliefs on models ignoring directionality. In Fig. 9, the difference between curves for the various sectors results from the different rates of occurrence of storms in those sectors.

We demonstrated above (e.g. Fig. 6) that the directional model provides better characterisation of extremal properties for the current hindcast data compared to a direction-independent model. Therefore, the directional model should be preferred for subsequent estimation and inference. There is no reason to expect that estimates for omni-directional design criteria derived from the directional model will be the same as those derived from the direction-independent model. Fitting a direction-independent model to data whose extremal behaviour varies with direction will usually underestimate extremes in some directions and overestimate in others. We cannot anticipate the overall bias on omni-directional design criteria introduced by modelling directionally varying extremes using a direction-independent model, other than by estimating design criteria using the appropriate directional model directly. For directional sectors corresponding to the most extreme storms, sector design criteria estimated using a directional model will be higher than those estimated using a direction-independent model. Conversely, for directional sectors corresponding to less extreme storms, sector design criteria estimated using a directional model will be lower than those estimated using a direction-independent model.

To illustrate this, consider a simple example. We observe data from a large number of independent storm peak events in a 10-year period, exactly half of which occur in directional sector [0, 180). By construction, in sector [0, 180), extremes follow a GPD with $\gamma = -0.2$, $\sigma = 2.4$ and threshold of 6 m, whereas in sector [180, 360) extremes follow a GPD with $\gamma = -0.4$, $\sigma = 2.4$ and threshold of 6 m. We estimate the most probable storm peak H_S

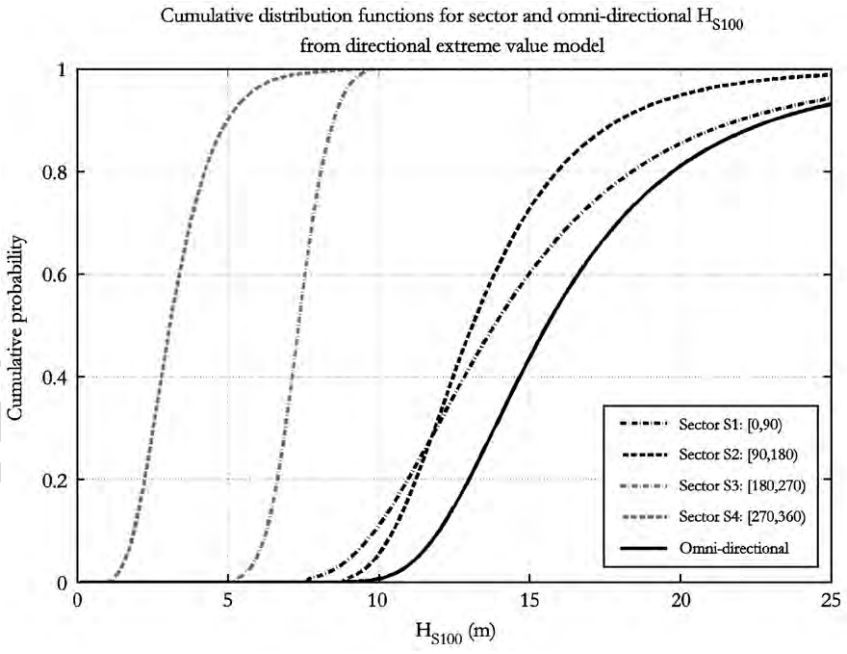

Fig. 8. Cumulative distribution functions for sector and omni-directional H_{S100} for GOMOS, using a first-order directional model for each of extreme value shape and scale.

corresponding to 100 years, using both a direction-independent model and a directional model (which models the homogeneous sectors independently). Results are illustrated (Fig. 10), as a function of the threshold assumed for modelling.

From the figure it is apparent that the estimate for the most probable value of H_{S100} from the directional model remains relatively constant with threshold. However, for the direction-independent model, the estimate varies with threshold, since the relative numbers of storms from the two sectors also varies with threshold. Thus, for any particular choice of threshold, the omni-directional estimates will be different in general. For thresholds above 12 m, no storms from sector [0, 180) remain in the sample for modelling (since the upper limit for a GPD with $\gamma = -0.4$, $\sigma = 2.4$ and threshold of 6 m is 12 m), and we

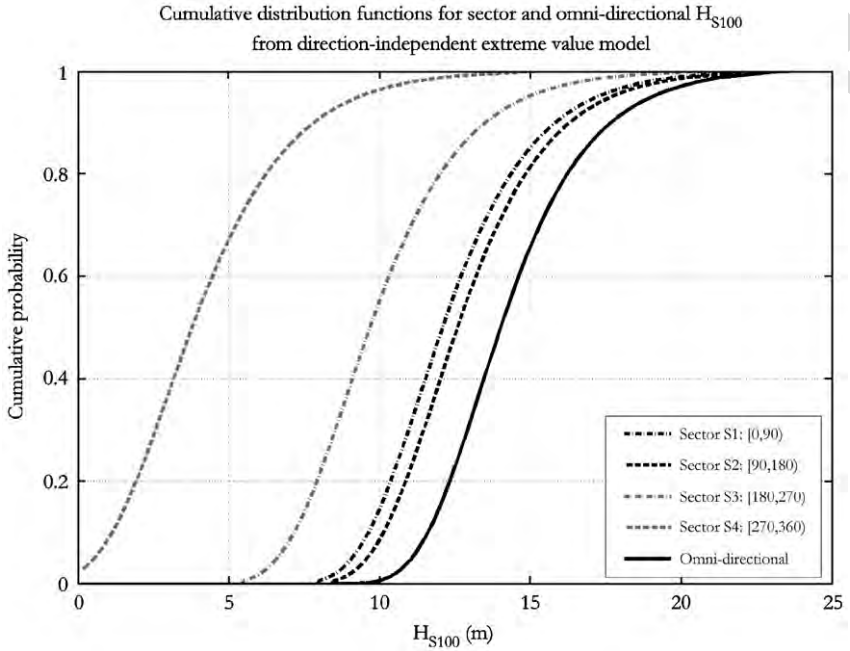

Fig. 9. Cumulative distribution functions for sector and omni-directional H_{S100} for GOMOS, using a directional-independent model for each of extreme value shape and scale. The omni-directional cumulant in particular is lighter tailed than the correspond cumulant in Fig. 8.

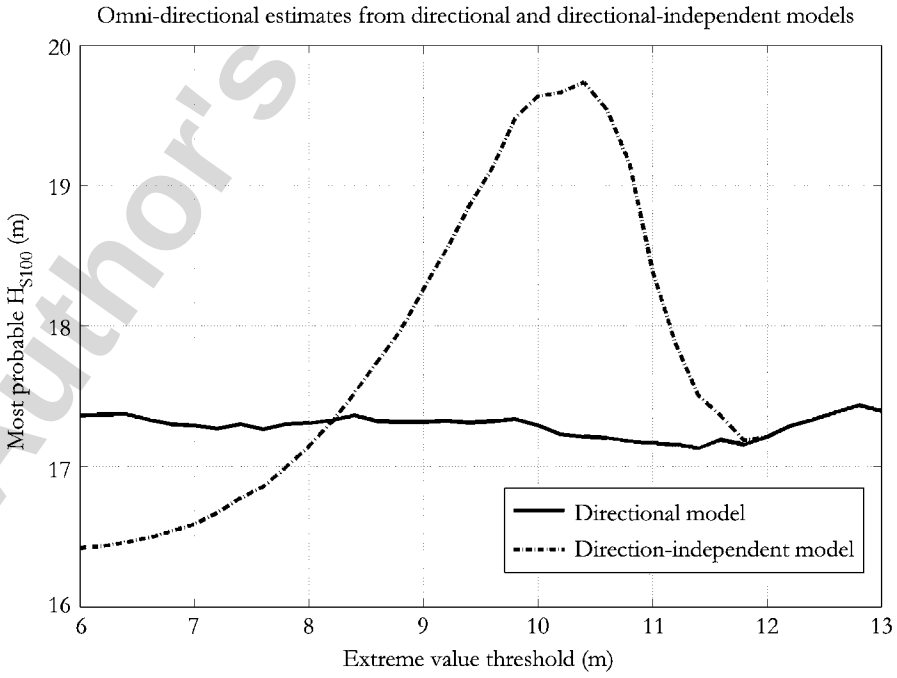

Fig. 10. Variation in most probable H_{S100} as a function of extreme value threshold, for simulated data modelled using either a directional or direction-independent model. The data for sectors [0,180) and [180,360) follow different GP distributions. Within each sector, data are homogeneous.

obtain consistent estimates. Of course, there is no reason to believe that a constant threshold should be applied with direction for extreme value modelling in general. Further, selecting a sufficiently high threshold to ensure appropriate estimates of the omni-directional extreme results in a considerably smaller sample for modelling, thereby inflating uncertainties of estimates.

5. Design criteria from directional extremes

We consider the specification of design criteria for directional extremes. First, we introduce three different approaches to directional design, consistent with a given omni-directional design criterion, and discuss their relative characteristics. We introduce a simple 2-sector application for illustrative purposes. Then we propose a risk-cost optimisation criterion to aid the selection of a balanced set of directional design criteria, accommodating both design risk and cost. The characteristics of the risk-cost optimised design are illustrated for the 2-sector problem. We calculate directional design criterion for the GOMOS location using each of the three-directional design approaches, for both the directional and direction-independent extreme value models discussed earlier.

Suppose we have a location at which occurrences of extremes storms can be partitioned with respect to direction into m directional sectors. Within each directional sector, extremes follow a common distribution, but the extreme value characteristics of the sectors are different. We wish to establish appropriate design criteria for each sector consistent with a given omni-directional non-exceedence probability $q_{100\,\mathrm{Omni}}$ at the 100-year return level. If design criteria are specified in terms of an omni-directional non-exceedence probability $q_{100\,\mathrm{Omni}}$, we can calculate the corresponding 100-year design H_S by inverting the equation $q_{100\,\mathrm{Omni}} = P(X_{\max\,100\,\mathrm{Omni}} \leqslant x_{100\,\mathrm{Omni}})$ to obtain $x_{100\,\mathrm{Omni}}$. However, specification of $q_{100\,\mathrm{Omni}}$ does not allow us to determine unique values for sector design H_S, but rather impose the constraint $q_{100\,\mathrm{Omni}} = \prod_{i=1}^{m} q_{100S_i}$, where q_{100S_i} are non-exceedence probabilities for the sectors $\{S_i\}_{i=1}^{m}$. That is, the product of sector non-exceedence probabilities must equal the omni-directional equivalent. This constraint leaves us free to specify any set of sector design H_S values $\{x_{100S_i}\}_{i=1}^{m}$ such that $q_{100S_i} = P(X_{\max 100S_i} \leqslant x_{100S_i})\ \ \forall i$ and $q_{100\,\mathrm{Omni}} = \prod_{i=1}^{m} q_{100S_i}$. An infinite number of solutions exist, but it is instructive to consider the following cases of interest.

(1) Suppose that all sectors but one exhibited extreme value behaviour with negative tail index, γ. For each of these sectors, an upper limit for the value of storm peak H_S therefore exists. It would therefore be possible to set the sector design values for all these sectors to their maximum value. The corresponding non-exceedence probabilities would all be unity. Then, $q_{100\,\mathrm{Omni}} = \prod_{i=1}^{m} q_{100S_i} = q_{100S^*}$, were S^* is the remaining sector with positive index. In this case, the omni-directional non-exceedence probability would correspond to that of the most extreme sector.

(2) Alternatively, we could design all sectors to a common design value x^* of H_S. The value of x^* to use must be chosen carefully, for example as motivated by the following considerations. For any sector, we define the distribution of the sector maximum H_S, $X_{\max\,100S_j}$, as

$$\begin{aligned} F_{X_{\max\,100S_j}}(x) &= P\Big(X_{\max\,100S_j} \leqslant x | X_i > u \forall i, \quad i \in [1,2,\ldots,n]\Big), \\ &= \prod_{i=1}^{n}\left\{\sum_{k=0}^{\infty} P\big(\rho_i(S_j) X_i \leqslant x | X_i > u, \quad M_i = k\big) \times P(M_i = k)\right\}, \\ &= \prod_{i\in S_j}\left\{\left\{\sum_{k=0}^{\infty} P(X_i \leqslant x | X_i > u, \quad M_i = k) \times P(M_i = k)\right\} A_{Sj}(x)\right\}, \end{aligned}$$

where

$$A_{Sj}(x) = \prod_{i\notin S_j}\left\{\sum_{k=0}^{\infty} P\big(\rho_i(S_j) X_i \leqslant x | X_i > u, \quad M_i = k\big) \times P(M_i = k)\right\} \in [0,1].$$

We define the distribution of the sector maximum storm peak H_S, $X^{\mathrm{SP}}_{\max\,100S_j}$, as

$$\begin{aligned} F_{X^{\mathrm{SP}}_{\max\,100S_j}}(x) &= P\Big(X^{\mathrm{SP}}_{\max\,100S_j} \leqslant x | X_i > u \quad \forall i, \\ &\qquad I \in [1,2,\ldots,n]\Big), \\ &= \prod_{i\in S_j}\left\{\sum_{k=0}^{\infty} P(X_i \leqslant x | X_i > u, \quad M_i = k) \, P(M_i = k)\right\}, \end{aligned}$$

obtaining $F_{X_{\max\,100S_j}}(x) = A_{Sj}(x) F_{X^{\mathrm{SP}}_{\max\,100S_j}}(x)$, so that $X_{\max 100S_j}$ has a heavier right-hand tail than $X^{\mathrm{SP}}_{\max 100S_j}$.

We define the distribution of the all-sector maximum H_S, $X_{\max\,100\,\mathrm{All}\,S}$, as

$$\begin{aligned} F_{X_{\max\,100\,\mathrm{All}\,S}}(x) &= \prod_{j=1}^{n_S} F_{X_{\max\,100S_j}}(x), \\ &= \prod_{j=1}^{n_S} A_{Sj}(x) F_{X^{\mathrm{SP}}_{\max\,100S_j}}(x), \\ &= \prod_{j=1}^{n_S} A_{Sj}(x) \prod_{j=1}^{n_S} F_{X^{\mathrm{SP}}_{\max\,100S_j}}(x), \end{aligned}$$

whereas the distribution of the omni-directionally maximum storm peak H_S is defined as

$$F_{X_{\max\ 100\ \mathrm{Omni}}}(x) = \prod_{i=1}^{n}\left\{\sum_{k=0}^{\infty} P(X_i \leqslant x | X_i > u, \quad M_i = k) \times P(M_i = k)\right\} = \prod_{j=1}^{n_S} F_{X^{\mathrm{SP}}_{\max\ 100 S_j}}(x).$$

Thus,

$$F_{X_{\max\ 100\ \mathrm{All}S}}(x) = \prod_{j=1}^{n_S} F_{X_{\max\ 100 S_j}}(x) \leqslant \prod_{j=1}^{n_S} F_{X^{\mathrm{SP}}_{\max\ 100 S_j}}(x), = F_{X_{\max\ 100\ \mathrm{Omni}}}(x).$$

We have equality in the last expression if and only if each storm influences only the sector in which its storm peak H_S occurs, i.e. $\rho_i(S_j) = 1$ iff $i = j$, otherwise $\rho_i(S_j) = 0$.

We could set the common sector design value x^* to the omni-directional 100-year H_S, $x_{100\ \mathrm{Omni}}$, defined using the expression $q_{100\ \mathrm{Omni}} = F_{X_{\max\ 100\ \mathrm{Omni}}}(x_{100\ \mathrm{Omni}})$ for storm peak data. Under the assumption that storms contribute to one and only one sector, this value of x^* would guarantee the correct omni-directional non-exceedence probability $q_{100\ \mathrm{Omni}}$. In general, setting the common sector design value $x^* = x_{100\ \mathrm{Omni}}$ would result in an all-sector non-exceedence probability $\tilde{q}_{100\ \mathrm{Omni}} = \prod_{i=1}^{n_S} q_{100 S_i} \leqslant q_{100\ \mathrm{Omni}}$. This in turn suggests setting $x^* \geqslant x_{100\ \mathrm{Omni}}$ to achieve the desired all-sector non-exceedence probability, but the appropriate value of x^* is now application-specific, dependent on the values of $\{\rho_i(S_j)\}_{i=1,\ j=1}^{n,m}$. For definiteness here, we consider the common sector design value $x^* = x_{100\ \mathrm{Omni}}$, and refer to this design as the "omni-directional H_{S100}" design. Fig. 11 illustrates this method of selection of sector design criteria in the case $m = 2$ for ease of discussion. In this example, sector $S1$ is more severe that sector $S2$. Naturally, sector design non-exceedence probabilities are both larger than the omni-directional value, but we note that the non-exceedence probability for the more severe sector ($S1$) is less than that for the less severe sector ($S2$). It is clear in general that sector non-exceedence probabilities $\{q_{100 S_i}\}_{i=1}^{m}$ will be very different to each other. Indeed, non-exceedence probabilities for the most severe sectors will always be lower that those for less severe sectors. But even for the most severe sector, the sector non-exceedence probability will always be at least as large as the omni-directional value.

(3) A third possibility is to maximise the value of the minimum sector non-exceedence probability. This is achieved by setting the same non-exceedence probability for each sector. In this case, we have $q_{100\ \mathrm{Omni}} = \prod_{i=1}^{m} q_{100S} = (q_{100S})^m$ where $q_{100S} = (q_{100\ \mathrm{Omni}})^{1/m}$ is the common sector non-exceedence probability. We refer to this design as the "equal sector non-exceedence" design. Fig. 12 illustrates the approach in the case $m = 2$. Now we impose more demanding non-exceedence requirements equally across all sectors, including

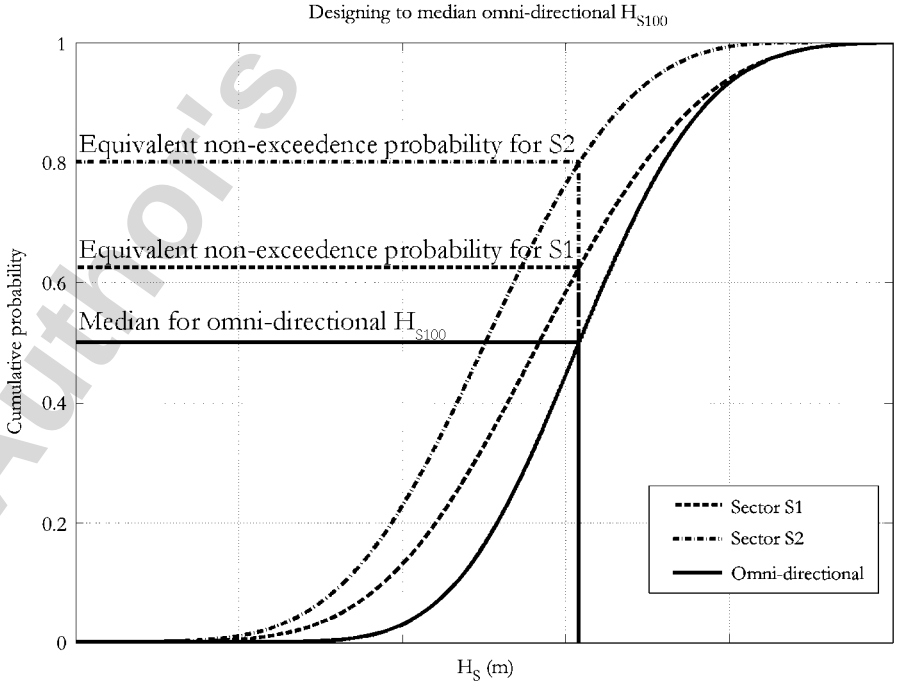

Fig. 11. Designing to median omni-directional H_{S100}, for the two-sector problem. The equivalent sector non-exceedence probability is smaller for the more severe sector.

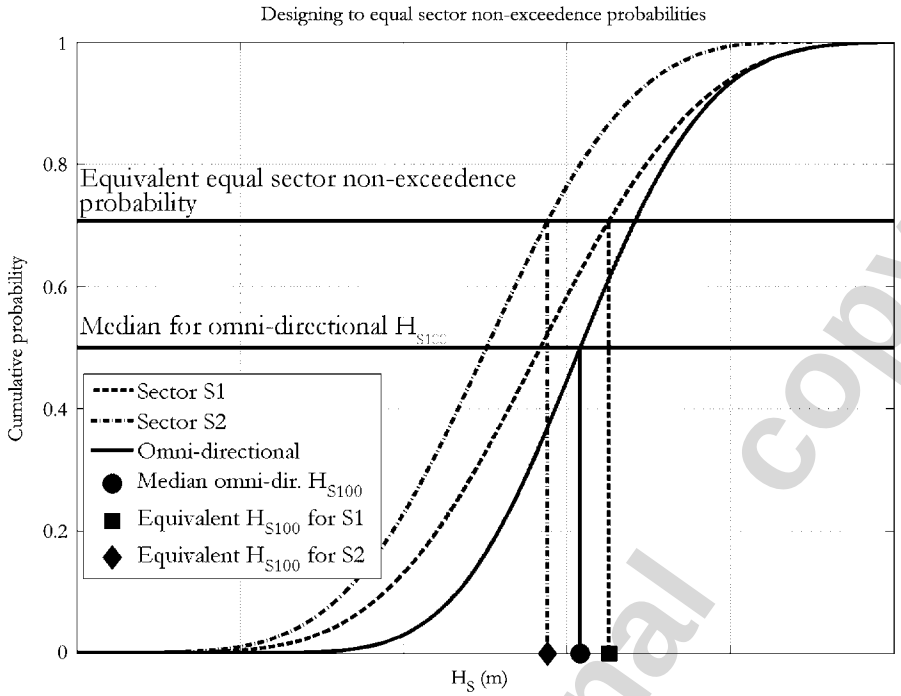

Fig. 12. Designing to equal non-exceedence probabilities for each sector, illustrated for the two-sector problem. The equivalent sector H_S for the more severe sector is larger than the omni-directional value.

the most severe. Note that, for any homogeneous sample size n corresponding to time period P_0 years, from a GPD with parameters γ and σ, we have $\frac{nP}{P_0}\left(1+\frac{\gamma}{\sigma}(x-u)\right)_+^{-1/\gamma} = -\ln q$ which defines the relationship between the P year non-exceedence probability q and extreme quantile x. Setting the extreme 100-year quantile using a non-exceedence probability $q^{1/m}$ (so that $\frac{100n}{P_0}\left(1+\frac{\gamma}{\sigma}(x-u)\right)_+^{-1/\gamma} = -\ln q^{1/m} = -\frac{1}{m}\ln q$) is equivalent to a non-exceedence probability q at the $100m$-year level. Thus, this approach sets $100\,m$-year return levels for each directional sector. Specifically, in the case $m = 8$ we would set 800-year return levels in each sector.

We see that the particular choices of $\{x_{100S_i}\}_{i=1}^m$ discussed above are valid, but have different characteristics and design consequences. We might judge, if we were to follow the third approach above, that setting the most extreme sector at the $100m$-year level was over-conservative. At the same time, we might like to introduce more conservatism for the most severe sector than that produced by the second approach above. For this reason, we might consider a risk-cost basis for optimisation of directional design criteria. If $c(x)$ is the cost of designing to a storm peak H_S of x metres, then the overall cost of design will be $\mathrm{RC} = \sum_{i=1}^m c(x_{100S_i})$, where $x_{100S_i} = x_{100S_i}(q_{100S_i})$ is the sector storm peak H_S corresponding to sector non-exceedence probability q_{100S_i}. The optimal design is that which mimises RC subject to $q_{100\,\mathrm{Omni}} = \prod_{i=1}^m q_{100S_i}$ where $q_{100\,\mathrm{Omni}}$ is some quantile (typically $\geqslant 0.5$) of the omni-directional cumulative distribution.

For our two-sector problem, Fig. 13 illustrates risk-cost optimisation. For simplicity, we assume that the cost of construction for either sector takes the form $c(x) = Kx^2$, for x in metres, where for convenience we set $c(10) = 1$, so that $K = 0.01$. We further set $q_{100\,\mathrm{Omni}} = 0.5$. We see that optimal risk-cost design corresponds to minimum total design cost given $q_{100\,\mathrm{Omni}} = 0.5$. The optimal risk-cost design (labelled "A") is a compromise between designing to the omni-directional H_S in all sectors (labelled "B"), and designing to equal non-exceedence probabilities in each sector (labelled "C").

Tables 2 and 3 present design criteria from the GOMOS data set, for design to non-exceedence probabilities of 0.5 and 0.7 for omni-directional H_{S100}, based on three design approaches and two extreme value models. The corresponding values for an annual probability of exceedance of 0.01 are given in Appendix B. Looking at Table 2 first, comparing the top and bottom halves of the table, we see that design values based on the directional model are larger that their counterparts obtained by ignoring the directional dependence of storms. This indicates that ignoring directionality results in underestimation of extreme storm behaviour. Results also illustrate the different characteristics of the three design approaches used. The risk-cost optimal design avoids the more extreme properties of the other design methods, such as the large range of values for $\{q_{100S_1}\}_{i=1}^m$ present for design to omni-directional H_{S100}, and the large range of values for $\{x_{100S_1}\}_{i=1}^m$ evident for design to equal sector non-exceedence.

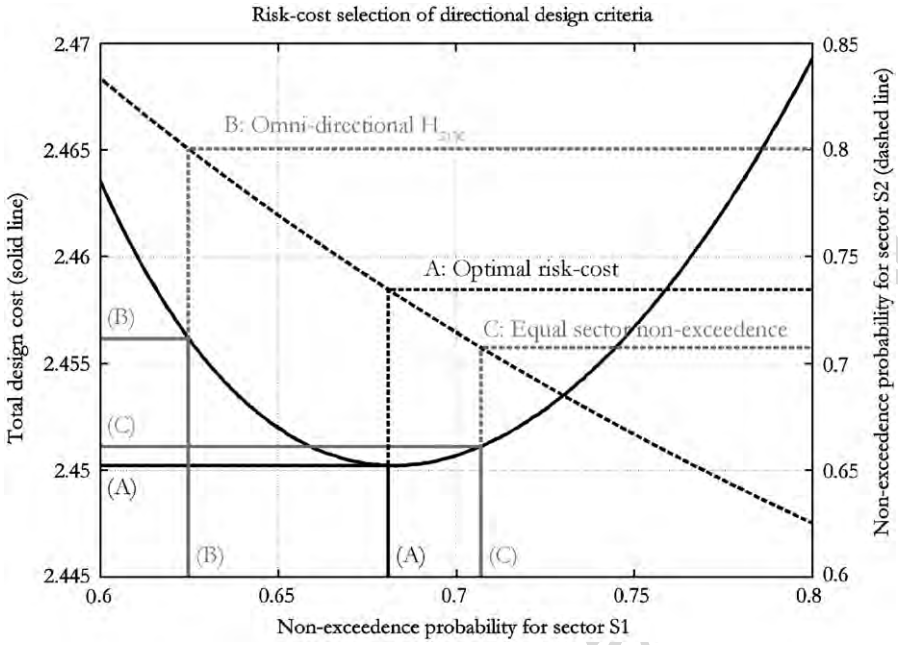

Fig. 13. Directional design criteria optimising risk-cost for the two-sector problem. Shown, as a function of non-exceedence probability for sector $S1$, are: total design cost (solid line, with ordinate on left-hand side) and corresponding non-exceedence probability for sector $S2$ (dashed line, with ordinate on right-hand side). The optimal design (labelled "A") minimises total design cost for a risk level quantified in terms of a non-exceedence probability for H_{S100} of $q_{100\,\mathrm{Omni}} = 0.5$. Also shown (in grey) are the "omni-directional H_{S100}" design (labelled "B") and the "equal sector non-exceedence" design (labelled "C").

Table 2
Design criteria based on median omni-directional H_{S100}

Sector	Angle	Risk-cost optimal			Omni-directional H_{S100}			Equal sector non-exceedence		
		RC	x_{100S_i}	q_{100S_i}	RC	x_{100S_i}	q_{100S_i}	RC	x_{100S_i}	q_{100S_i}
Directional model										
$S1$	[0,90)	8.78	18.03	0.75	9.73	15.60	0.59	9.29	20.20	0.84
$S2$	[90,180)		17.40	0.81		15.60	0.69		17.90	0.84
$S3$	[180,270)		11.44	0.91		15.60	0.98		10.30	0.84
$S4$	[270,360)		10.90	0.90		15.60	0.98		9.70	0.84
Direction-independent model										
$S1$	[0,90)	7.56	15.00	0.82	7.84	14.00	0.72	7.59	15.20	0.84
$S2$	[90,180)		15.40	0.82		14.00	0.66		15.70	0.84
$S3$	[180,270)		13.41	0.84		14.00	0.88		13.40	0.84
$S4$	[270,360)		10.67	0.89		14.00	0.98		10.10	0.84

Taking the risk-cost optimal design based on the directional EV model to be most preferable, we conclude that we need to design for 18 m in sector S1, 17.4 m in S2, but only 11.4 and 10.9 m, respectively, in sectors S3 and S4. We note that the all-sector non-exceedence probabilities $\tilde{q}_{100\,\mathrm{Omni}}$ corresponding to the omni-directional H_{S100} for both the directional (e.g. $0.59 \times 0.69 \times 0.98 \times 0.98 = 0.39$) and directional independent models is less that 0.5, whereas the omni-directional non-exceedence probabilities corresponding to the risk-cost and equal sector non-exceedence criteria are both equal to 0.5. This is consistent with the argument presented at the beginning of this section and reflects the fact that a given storm contributes to extremes in more that one sector in general. We have further estimated that adjusted "omni-directional H_{S100}"values of 16.7 m (directional model) and 14.5 m (direction-independent model) would be required to achieve $\tilde{q}_{100\,\mathrm{Omni}} = 0.5$.

In addition to reflecting the trends of the previous table, Table 3 quantifies the extent to which basing design on H_{S100} non-exceedence probability of 0.7 increases design values for all models and design methods, and for the chosen risk-cost optimal design based on the directional EV model in particular. We note again that all-sector non-exceedence probabilities $\tilde{q}_{100\,\mathrm{Omni}}$ corresponding to the omni-directional H_{S100} for both the directional (e.g. $0.74 \times 0.84 \times 0.99 \times 0.99 = 0.61$) and directional-independent models is less that 0.7, whereas the all-sector exceedence probabilities corresponding to the risk-cost

Table 3
Design criteria based on omni-directional H_{S100} non-exceedence of 0.7

Sector	Angle	Risk-cost optimal			Omni-directional H_{S100}			Equal sector non-exceedence		
		RC	x_{100S_i}	q_{100S_i}	RC	x_{100S_i}	q_{100S_i}	RC	x_{100S_i}	q_{100S_i}
Directional model										
*S*1	[0,90)	11.55	20.97	0.86	12.82	17.90	0.74	12.20	23.40	0.92
*S*2	[90,180)		19.67	0.90		17.90	0.84		20.20	0.92
*S*3	[180,270)		12.92	0.95		17.90	0.99		11.60	0.92
*S*4	[270,360)		12.70	0.95		17.90	0.99		11.40	0.91
Direction-independent model										
*S*1	[0,90)	8.99	16.30	0.91	9.36	15.30	0.85	9.03	16.50	0.91
*S*2	[90,180)		16.70	0.90		15.30	0.81		17.00	0.92
*S*3	[180,270)		14.70	0.91		15.30	0.94		14.70	0.91
*S*4	[270,360)		11.76	0.94		15.30	0.99		11.20	0.91

and equal sector non-exceedence criteria are both equal to 0.7. We have further estimated that adjusted "omni-directional H_{S100}"values of 19.1 m (directional model) and 15.8 m (direction-independent model) would be required to achieve $\tilde{q}_{100\,\mathrm{Omni}} = 0.7$.

6. Conclusions and recommendations

Directional metocean data allow the possibility for directionality to be taken into account in the design of offshore structures, but care must be taken to ensure that models and design criteria are developed and applied consistently.

A directional extremes model (a Fourier series expansion here) allows directionally consistent extreme values to be developed, with obvious applicability for engineering design. There is a strong general case in favour of adopting a directional extreme value model to storm peak H_S data unless it can be demonstrated statistically that a direction-free model is no less appropriate. For the current GOMOS hindcast sample, a directional GPD model explains the data significantly better than the conventional (direction-free) model. A first-order Fourier series model was found adequate for the GOMOS data analysed, but we expect that higher order models might be necessary for locations with more complex directionality.

It is important to consider the directionality of sea states when developing extremal criteria. Omni-directional extreme values derived from a directional model are different in general from those obtained from a direction-independent derivation, which ignores the distribution variability of the data with direction. For example, when the directional dependence of the GOMOS data is modelled with a Fourier series expansion, the omni-directional H_{S100} is heavier tailed than that derived from a direction-independent approach, indicating that large values of H_{S100} are more likely than we might anticipate were we to base our beliefs on EV models which ignore directionality.

In this work, we model extremal properties of storm peak H_S as a function of wave direction at storm peak, taking each storm event to be independent statistically for a given location. We therefore ignore all but the most severe 30-min sea state of the storm for extreme value analysis. In estimating maximum storm H_S for a directional sector, we accommodate the effects of all sea states of all storms whose wave directions fall within that directional sector, regardless of the wave direction at storm peak, by quantifying the directional influence of storms on the directional sector directly from the data.

The rate of occurrence of storms peaks is dependent on storm peak direction in general. Hence, the distribution of H_{S100} will have storm peak directional dependence in general, even when the extremal value characteristics (e.g. GPD shape and scale) of storm peak H_S are independent of storm peak direction. The evidence from the current GOMOS data is that the rate of occurrence of storms shows strong storm peak directional dependence.

The process of setting criteria for a number of directional sectors for a given omni-directional non-exceedance probability is not unique. Nevertheless, directional design criteria provide more specific estimates of extreme offshore conditions enabling the risk associated with a design to be minimised given available resources. We propose a risk-cost basis as an objective method for optimising directional criteria, while preserving overall reliability. The risk-cost optimal design avoids more extreme properties of the other design methods, such as the large range of values of sector non-exceedance probabilities in the design to omni-directional value, or the large range of sector extremes in the design to equal sector non-exceedances.

The analysis presented here provides estimates for the full probability distribution of extreme quantiles such as H_{S100}, for directional sectors and omni-directionally, in addition of point estimates such as the median or most probable values. This offers the engineer the opportunity to design structures via a full directional reliability analysis, by first estimating structural failure probability per

directional sector, and then multiplying directional failure probabilities to estimate overall reliability.

Acknowledgements

The authors acknowledge the support of Shell International Exploration and Production and Shell Research Limited for this work. The authors acknowledge useful discussions with George Forristall and Michael Vogel, the assistance of Joost den Haan in data handling and computing support, and useful comments from three reviewers.

Appendix A. Maximum likelihood estimation for the directional model

The probability density function for each of the set $\{X_i\}_{i=1}^n$ of storm peak significant wave heights following a GPD introduced in Section 3 is

$$f_{X_i|\theta_i,u}(x) = \frac{1}{\sigma_i}\left(1+\frac{\gamma_i}{\sigma_i}(x-u)\right)_+^{-(1/\gamma_i)-1},$$

for $x>u$, $\sigma>0$.

The likelihood of a data sample $\{X_i\}_{i=1}^n$ is given by

$$L\left(\{A_{abk}\};\{X_i\}_{i=1}^n\right) = \prod_{i=1}^n \frac{1}{\sigma_i}\left(1+\frac{\gamma_i}{\sigma_i}(X_i-u)\right)_+^{-(1/\gamma_i)-1}$$

and the negative log likelihood by $l=\sum_{i=1}^n l_i$, where

$$l_i = \log\,\sigma_i + \left(\frac{1}{\gamma_i}+1\right)\log\left(1+\frac{\gamma_i}{\sigma_i}(X_i-u)\right)_+,$$

where $\gamma_i=\gamma(\theta_i)$, $\sigma_i=\sigma(\theta_i)$, $i=1,2,\ldots,n$.

Thus,

$$\frac{\partial l_i}{\partial \gamma_i} = -\frac{1}{\gamma_i^2}\left(\log\,G_i - (1+\gamma_i)\left(1-\frac{1}{G_i}\right)\right)$$

and

$$\frac{\partial l_i}{\partial \sigma_i} = -\frac{1}{\gamma_i\sigma_i} + \frac{1}{\sigma_i}\left(1+\frac{1}{\gamma_i}\right)\frac{1}{G_i},$$

where

$$G_i = \left(1+\frac{\gamma_i}{\sigma_i}(X_i-u)\right)_+.$$

Maximum likelihood (or minimum negative log likelihood) estimates are found by setting the partial derivatives of l with respect to the parameter set A_{110}, A_{210}, A_{abk}, $a=1,2$, $b=1,2$, $k=1,2,\ldots,p$ equal to 0. Given the Fourier series form $\sum_{k=0}^p\sum_{b=1}^2 A_{abk}t_b(k\theta)$ with $a=1$ for γ, and $a=2$ for σ, we can write

$$\frac{\partial l}{\partial A_{abk}} = \sum_{i=1}^n U_{ai}t_b(k\theta_i),$$

$a=1,2$, $b=1,2$, $k=0,1,\ldots,p$ where $U_{ai}=\partial l_i/\partial\gamma$ for $a=1$, and $\partial l_i/\partial\sigma$ for $a=2$, recalling that $A_{a20}\triangleq 0$.

Second derivatives of the likelihood can be found by applying the chain rule to the expressions above for first derivatives. The identities

$$E_X\left[\left(1+\frac{\gamma}{\sigma}(X-u)\right)_+^{-r}\right] = \frac{1}{1+\gamma r}$$

for $1+\gamma r>0$, (which can be evaluated directly using $E_X(g(X))=\int g(x)f_X(x)\,\mathrm{d}x$ and $E_X[(\log(1+(\gamma/\sigma)(X-u))_+)^r]=(-\gamma)^r\Gamma(r+1)$ for integer r, (which can be evaluated directly, noting e.g. the similarity the integrand with the density of the gamma random variable), when $X\sim\mathrm{GPD}(\gamma,\sigma)$ are required, yielding the expectations:

$$E_X\left[\frac{\partial^2 l}{\partial A_{abk}\,\partial A_{\alpha\beta\kappa}}\right] = \sum_{i=1}^n \frac{B_{a\alpha i}}{C_i}t_b(k\theta_i)t_\beta(\kappa\theta_i),$$

$\forall a,b,k,\alpha,\beta,\kappa,$

where

$$B_{a\alpha i} = \begin{Bmatrix} 2\sigma^2(\theta_i), & a=\alpha=1 \\ (1+\gamma(\theta_i)), & a=2,\ \alpha=1 \\ \sigma(\theta_i), & a=\alpha=2 \end{Bmatrix}$$

and

$$C_i = \sigma^2(\theta_i)(1+\gamma(\theta_i))(1+2\gamma(\theta_i)), \quad \forall i.$$

The asymptotic variances for parameter estimates can be read from the asymptotic covariance matrix for parameter estimates, given by the inverse I^{-1} of the information matrix:

$$I = E_X\left[\left\{\frac{\partial^2 l}{\partial A_{abk}\,\partial A_{\alpha\beta\kappa}}\right\}\right].$$

Moreover, the asymptotic variance of a function $g(\{A_{abk}\})$ of the parameters is given by

$$var_A(g(\{A_{abk}\})) = \left[\frac{\partial g}{\partial A_{abk}}\right]' I^{-1}\left[\frac{\partial g}{\partial A_{abk}}\right],$$

where $[\partial g/\partial A_{abk}]$ represents a vector with elements $\{\partial g/\partial A_{abk}\}$. Thus, asymptotic variances for functions of the parameters, e.g. H_{S100}, can be derived. Asymptotic variances for parameter estimates facilitate a studentised bootstrapping resampling analysis (see, e.g. Jonathan and Ewans, 2006), which allows reliable interval estimates for parameters to be calculated.

Table B1
Low and high bootstrap confidence interval exceedance probabilities for the independent (I), dependent (D) and resample (R) cases

Parameter	I:Low	I:High	D:Low	D:High	R:Low	R:High
$A110$	0.09	0.01	0.05	0.04	0.06	0.06
$A111$	0.05	0.02	0.06	0.04	0.04	0.12
$A121$	0.02	0.06	0.07	0.05	0.05	0.08
$A210$	0.01	0.10	0.04	0.05	0.06	0.03
$A211$	0.03	0.03	0.05	0.05	0.13	0.02
$A221$	0.09	0.02	0.06	0.03	0.07	0.04

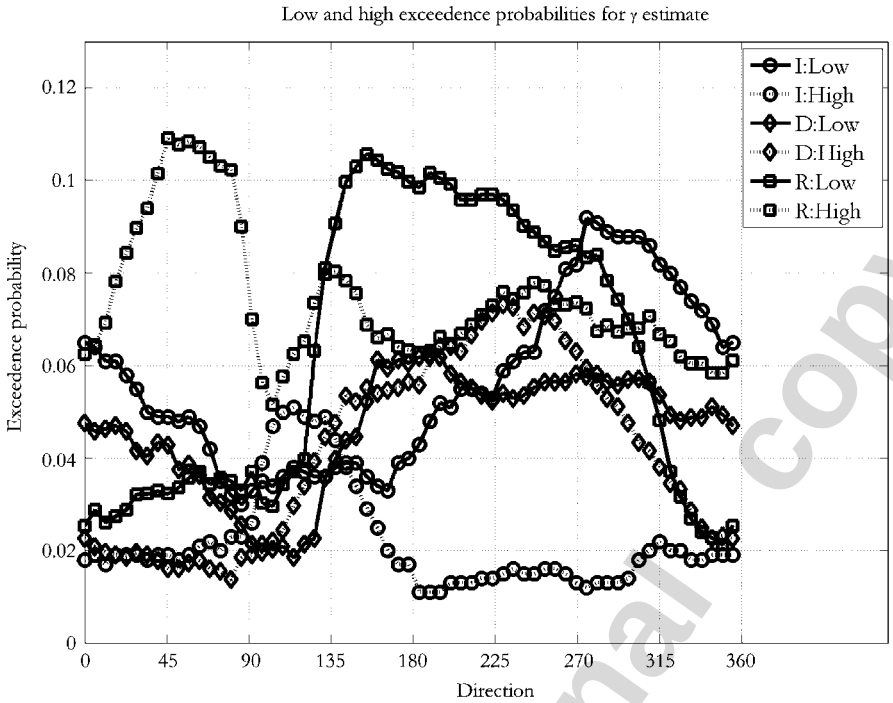

Fig. B1. Low and high bootstrap confidence interval exceedance probabilities of γ for the independent (I), dependent (D) and resample (R) cases.

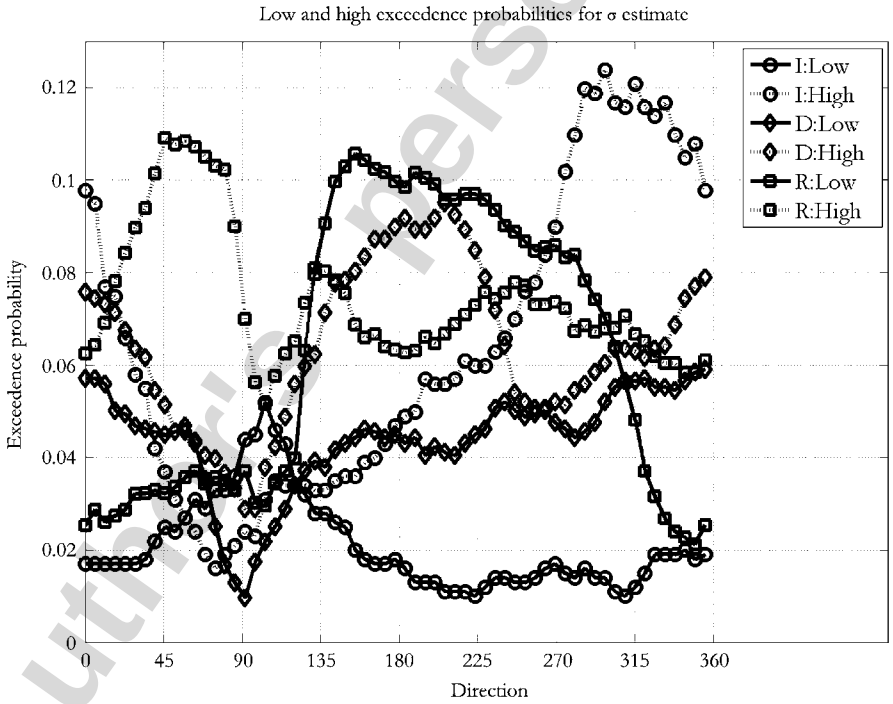

Fig. B2. Low and high bootstrap confidence interval exceedance probabilities of σ for the independent (I), dependent (D) and resample (R) cases.

Appendix B. Coverage performance of bootstrap interval estimates for parameters of cyclic model

The coverage performance of bootstrap interval estimates for the parameters of the first-order cyclic models for extreme value shape and scale parameters was evaluated for three different cases (independent (I), dependent (D) and resample (R)), when the true data model is known. The motivation for the study was to ensure that bootstrap interval estimates are realistic for different spatial dependency between locations.

We performed the following simulation study. Data samples of size 315 storms for 120 locations were generated using the first-order cyclic model (for each of extreme value shape and scale) with parameters estimated using the true GOMOS data (and given in Table 1) for each location, for

Table C1
Design criteria based on omni-directional H_{S100} non-exceedence of 0.37

Sector	Angle	Risk-cost optimal			Omni-directional H_{S100}			Equal sector non-exceedence		
		RC	x_{100S_i}	q_{100S_i}	RC	x_{100S_i}	q_{100S_i}	RC	x_{100S_i}	q_{100S_i}
Directional model										
*S*1	[0,90)	7.55	16.60	0.67	8.29	14.40	0.48	8.03	18.60	0.78
*S*2	[90,180)		16.20	0.74		14.40	0.56		16.80	0.78
*S*3	[180,270)		10.80	0.88		14.40	0.97		9.80	0.78
*S*4	[270,360)		10.04	0.86		14.40	0.97		8.90	0.78
Direction-independent model										
*S*1	[0,90)	6.83	14.29	0.76	7.08	13.30	0.63	6.85	14.50	0.78
*S*2	[90,180)		14.70	0.75		13.30	0.55		15.00	0.78
*S*3	[180,270)		12.70	0.78		13.30	0.83		12.70	0.78
*S*4	[270,360)		10.05	0.84		13.30	0.97		9.40	0.78

three different situations. In the first case (independent), independent data samples were generated for each location. In the second case, (dependent), identical data were used for each location for any given storm. In the third case, (resample), a resample (storm-wise across all locations) of the actual GOMOS data was used. The independent and dependent cases correspond to limiting dependence structures that we would encounter in practice.

For at least 1000 realisations of the data, 200 bootstrap samples were used to estimate extreme value parameter uncertainty. Results are given in Table B1 below, in terms of fraction of realisations for which the real parameter values of the first-order cyclic model fall outside of the bootstrap interval estimate on the left- and right-hand sides. (The actual number of realisations used for each of independent, dependent and resample studies was 1000, 1700 and 1500, respectively, due to different computational requirements and computing resources devoted to the different simulations).

In the table, we expect total exceedance probability to be 0.05, since we are using a 95% interval, with 0.025 exceedance probabilities on each of the left- and right-hand sides. Values in Table B1 confirm that the bootstrap confidence interval estimate is performing adequately in all three cases; numbers of exceedances are generally consistent with expectation. Figs. B1 and B2 illustrate low and high bootstrap confidence interval exceedance probabilities for extreme value shape and scale as a function of storm peak direction. Again, results are broadly consistent with expectation.

We conclude from these simulation studies that the bootstrap interval estimates for cyclic model parameters, and model parameter variability with storm peak direction, are realistic.

Appendix C. Design criteria based on omni-directional H_{S100} non-exceedence of 0.37 (annual probability of non-exceedance of 0.99)

Design criteria based on omni-directional H_{S100} non-exceedence of 0.37 (Table C1).

References

Arena, F., Meduri, S., Pavone, D., Romolo, A., 2006. Directional return period of severe storms off Italian coasts. In: Proceedings of the 25th International Conference on Offshore Mechanics and Arctic Engineering, June 4–8, 2006, Hamburg, Germany, OMAE2006-92615.

Casson, E., Coles, S.G., 1999. Spatial regression models for extremes. Extremes 1, 449.

Chavez-Demoulin, V., Davison, A.C., 2005. Generalized additive modelling of sample extremes. Journal of the Royal Statistical Society. Series C: Applied Statistics 54 (1), 207–222.

Coles, S.G., Casson, E., 1998. Extreme value modelling of hurricane wind speeds. Structural Safety 20, 283.

Coles, S.G., Powell, E.A., 1996. Bayesian methods in extreme value modelling: a review and new developments. International Statistics Review 64, 119.

Coles, S., Simiu, E., 2003. Estimating uncertainty in the extreme value analysis of data generated by a hurricane simulation model. Journal of Engineering Mechanics 129, 1288–1294.

Coles, S.G., Tawn, J.A., 1996. A Bayesian analysis of extreme rainfall data. Applied Statistics 45, 463.

Coles, S.G., Tawn, J.A., 2005. Bayesian modelling of extreme sea surges on the UK east coast. Philosophical Transactions of the Royal Society A 363, 1387.

Coles, S.G., Walshaw, D., 1994. Directional modelling of extreme wind speeds. Applied Statistics 43, 139.

Davison, A.C., Hinkley, D.A., 1997. Bootstrap Methods and their Application. Cambridge Series in Statistical and Probabilistic Mathematics. Cambridge University Press, Cambridge, UK.

Efron, B., Tibshirani, R.J., 1993. An Introduction to the Bootstrap. Chapman & Hall, New York.

Elsinghorst, C., Groeneboom, P., Jonathan, P., Smulders, L., Taylor, P.H., 1998. Extreme value analysis of North Sea storm severity. Journal of Offshore Mechanics Ocean Engineering 120, 177.

Ewans, K.C., Jonathan, P., 2007. The effect of directionality on Northern North Sea extreme wave design criteria. In: Proceedings of the 26th International Conference on Offshore Mechanics and Arctic Engineering, June 10–15, 2007, San Diego, USA, OMAE2007-29657.

Forristall, G.Z., Larrabee, R.D., Mercier, R.S., 1991. Combined oceanographic criteria for deepwater structures in the Gulf of Mexico. In: Offshore Technology Conference Proceedings, OTC 6541, Houston.

Forristall, G.Z., 2004. On the use of directional wave criteria. Journal of Waterway, Port, Coastal and Ocean Engineering 130, 272.

Hall, P., 1988. The Bootstrap and Edgeworth Expansion. Springer, New York.

Heffernan, J.E., Tawn, J.A., 2004. A conditional approach for multivariate extreme values. Journal of the Royal Statistical Society B 66, 497–546.

Jonathan, P., Ewans, K.C., 2006. Uncertainties in extreme wave height estimates for hurricane dominated regions. In: Proceedings of the 25th International Conference on Offshore Mechanics and Arctic Engineering, June 4–8, 2006, Hamburg, Germany.

Kotz, S., Nadarajah, S., 2000. Extreme Value Distributions: Theory and Applications. Imperial College Press, London, UK.

Leadbetter, M.R., Lindgren, G., Rootzen, H., 1983. Extremes and Related Properties of Random Sequences and Series. Springer, New York, USA.

Pickands, J., 1975. Statistical inference using extreme order statistics. Annals of Statistics 3, 119.

Oceanweather Inc., 2005. GOMOS—USA Gulf of Mexico Oceanographic Study, Northern Gulf of Mexico Archive, October 2005.

Reiss, R.D., Thomas, M., 2001. Statistical Analysis of Extreme Values. Birkhauser Verlag, Basel, Switzerland.

Robinson, M.E., Tawn, J.A., 1997. Statistics for extreme sea currents. Applied Statistics 46, 183.